Applied and Environmental Microbiology, Aug. 2007, p. 4959–4965 Vol. 73, No. 15
0099-2240/07/$08.00+0 doi:10.1128/AEM.02993-06

Cloning of a Novel Aldo-Keto Reductase Gene from *Klebsiella* sp. Strain F51-1-2 and Its Functional Expression in *Escherichia coli*[▽]

Hong Jiang,[1]† Chao Yang,[1,2]† Hong Qu,[3] Zheng Liu,[1,2] Q. S. Fu,[4] and Chuanling Qiao[1]*

State Key Laboratory of Integrated Management of Pest Insects & Rodents, Institute of Zoology, Chinese Academy of Sciences, Beijing 100101, China[1]; Graduate School of the Chinese Academy of Sciences, Beijing 100049, China[2]; College of Life Sciences, Peking University, Beijing 100871, China[3]; and Department of Civil and Environmental Engineering, Stanford University, Stanford, California 94305-4020[4]

Received 26 December 2006/Accepted 31 May 2007

A soil bacterium capable of metabolizing organophosphorus compounds by reducing the P═S group in the molecules was taxonomically identified as *Klebsiella* sp. strain F51-1-2. The gene involved in the reduction of organophosphorus compounds was cloned from this strain by the shotgun technique, and the deduced protein (named AKR5F1) showed homology to members of the aldo-keto reductase (AKR) superfamily. The intact coding region for AKR5F1 was subcloned into vector pET28a and overexpressed in *Escherichia coli* BL21(DE3). Recombinant His_6-tagged AKR5F1 was purified in one step using Ni-nitrilotriacetic acid affinity chromatography. Assays for cofactor specificity indicated that reductive transformation of organophosphorus compounds by the recombinant AKR5F1 specifically required NADH. The kinetic constants of the purified recombinant AKR5F1 toward six thion organophosphorus compounds were determined. For example, the K_m and k_{cat} values of reductive transformation of malathion by the purified recombinant AKR5F1 are 269.5 ± 47.0 μM and 25.7 ± 1.7 min^{-1}, respectively. Furthermore, the reductive transformation of organophosphorus compounds can be largely explained by structural modeling.

Synthetic organophosphorus (OP) compounds are widely used in agriculture to control major insect pests. These compounds have been implicated in several nerve and muscular diseases in human beings. Microbial degradation of OP pesticide has become the focus of many studies because it is economical and effective (30). The most widely studied bacterial enzyme for OP detoxification is the OP hydrolase (OPH). OPH has been isolated from several bacteria (23, 29), and the OPH from *Pseudomonas diminuta* has the widest range of substrate specificity (6). A similar enzyme, OPH A (OPDA), has been isolated from *Agrobacterium radiobacter* and was found to have 90% homology to OPH at the amino acid level (16). However, the rates of hydrolysis by OPH differ dramatically for members of the OP compound family, ranging from the diffusion-controlled limit for hydrolysis of paraoxon to several orders of magnitude slower for malathion, chlorpyrifos, and VX (6).

Various attempts have been made to isolate malathion-degrading microorganisms. Matsumura et al. isolated a malathion-degrading fungus, *Trichoderma viride*, and a bacterium, *Pseudomonas* sp., from contaminated soil, which rapidly degrades malathion through carboxylesteratic hydrolysis as well as desmethylation processes (22). Lewis et al. isolated a fungus, *Aspergillus oryzae*, from a freshwater pond, which transforms malathion to β-malathion monoacid and malathion dicarboxylic acid, indicating the presence of carboxylesteratic hydrolysis activity (19). Degradation of malathion by other bacterial species was also reported (11). Although many studies have been carried out on the microbial degradation of malathion, there is a lack of information on the genetic and enzymatic aspects in the degradation of malathion.

The aldo-keto reductases (AKRs) are a growing superfamily of approximately 120 enzymes, currently composed of 15 families from a wide variety of plants, animals, and prokaryotes (17). They catalyze the reversible NAD(P)H-dependent reduction of a wide range of ketones and/or aldehydes containing substrates including aliphatic and polycyclic aldehydes, aldoses, and lipid-derived aldehydes to the corresponding alcohols, which are endogenously produced intermediates in many metabolic pathway (20) and involved in the detoxification of carbonyl group-containing xenobiotics (2); methylglyoxal (39); antiemetic, antitumor drugs, and the carcinogen 4-methylnitrosamino-1-(3-pyridyl)-1-butanone NNK (1, 21); polycyclic aromatic hydrocarbons (5); and naloxone, naltrexone, and dihydromorphinone (40). The AKR superfamily is also found in a wide range of microorganisms, and the well-reported superfamily members include the xylose reductases, 2,5-diketo-D-gluconic acid reductases (2,5-DKGR A), and β-keto ester reductases, etc. These enzymes can metabolize many endogenous intermediate products, such as aldehydes and ketones, and exogenous compounds, including plant phytoallexins, toxins, and anthropogenic chemicals in the environment, as well as aldehydic products of lipid peroxidation (7). However, members of the AKR superfamily capable of metabolizing exogenous OP compounds have not been reported to date.

In the present study, a gene homologous to the AKR superfamily and responsible for the reduction of malathion as well as other thion OP compounds was cloned from a soil bacterium and expressed in *Escherichia coli*. Kinetic constants of the recombinant enzyme were also determined against various OP compounds.

* Corresponding author. Mailing address: State Key Laboratory of Integrated Management of Pest Insects & Rodents, Institute of Zoology, Chinese Academy of Sciences, Beijing 100101, China. Phone: 86-10-64807191. Fax: 86-10-64807099. E-mail: qiaocl@ioz.ac.cn.
† H.J. and C.Y. contributed equally to this work.
▽ Published ahead of print on 15 June 2007.

TABLE 1. Bacterial strains and plasmids used in this study

Strain or plasmid	Relevant characteristic(s)[a]	Source
Strains		
E. coli DH5α	Host for complementation cloning vectors	Tiangen
E. coli BL21(DE3)	Host for complementation expression vectors	Tiangen
Klebsiella sp.	Natural OP-degrading bacterium	This study
Plasmids		
pBluescript II SK(+)	Cloning vector, Ap^r	Novagen
pET28a(+)	Overexpression vector for His-Bind fusion proteins, Km^r	Novagen
pRA	Gene homologous to 2,5-diketo-D-gluconic acid reductase A of *E. coli* CFT073 in pET28a(+)	This study
pR	Gene homologous to putative AKR of *E. coli* CFT073 in pET28a(+)	This study

[a] Ap, ampicillin; Km, kanamycin.

MATERIALS AND METHODS

Bacterial strains, plasmids, and culture conditions. The bacterial strains and plasmids used in this study are listed in Table 1. *Escherichia coli* strains were grown on Luria-Bertani medium at 37°C. Ampicillin was used at 100 μg/ml and kanamycin at 50 μg/ml. Strain F51-1-2 was isolated from OP-contaminated soils using basal medium supplemented with trace elements (31) and 100 μg/ml malathion. Glucose was added at 1 g/liter as the carbon source. Moreover, the ability of strain F51-1-2 to metabolize OPs was confirmed by gas chromatogram under the same culture conditions.

Bacterial identification. Strain F51-1-2 was identified with reference to *Bergey's Manual of Determinative Bacteriology* (13). The BIOLOG bacterial identification test kit (Biolog, Inc., Hayward, CA) was used to test the ability of the isolate to utilize (oxidize) various carbon sources, and the procedures were followed according to the commercial protocol. The 16S rRNA gene of the strain was amplified by PCR (Perkin-Elmer PE9600 thermocycler) from chromosomal DNA, extracted by the method of Gardiner et al. (9) by using the 8f and 1512r universal primers (35). The PCR products were gel purified using QIAquick gel extraction kits (Tiangen), ligated into pMD18-T simple vector (TaKaRa), and sequenced (Invitrogen, Shanghai, China).

Cloning an *akr5f1* gene and data analysis. Routine DNA manipulations were carried out as described by Sambrook et al. (26). A size-fractionated genomic library was constructed from 4- to 10-kb DNA fragments (obtained from a partial Sau3AI digest) cloned into the BamHI site of plasmid pBluescript KS II (pBS) and transformed into *E. coli* DH5α (16, 43). Screenings for positive clones were performed spectrophotometrically by monitoring the absorbance at 410 nm resulting from the free thiol group produced from the P═S reduction of malathion (16, 18), and the inserted fragment from a positive clone was sequenced (Invitrogen). BlastN was used for the nucleotide sequence identity search, and BLASTP was used for the deduced amino acid identity search (www.ncbi.nlm.nih.gov/BLAST). Open reading frames (ORFs) were identified using the NCBI ORF finder tool. Promoter prediction was done online (www.fruitfly.org/seq_tools/promoter.html). The 5′ region of the deduced AKR gene was checked for the presence of ribosome binding site as described by Stormo et al. (32). Multiple alignments of amino acid sequences, construction of a neighbor-joining phylogenetic tree with a homology rate model, and a bootstrap analysis for evaluation of the phylogenetic topology were accomplished by using the Clustal X program (33) and MEGA 3 software (www.megasoftware.net).

Plasmid construction for overexpression in *E. coli*. Based on the two deduced ORFs, ra and r, in the sequenced fragment, oligonucleotide primers were synthesized to amplify the intact coding regions. The restriction sites for EcoRI and HindIII (underlined) were incorporated into the forward and the reverse primer sequences, respectively. The following two pairs of primers were used: pair I (forward, 5′ GGCGAATTCATGCAAACTGTAAAAC 3′; reverse, 5′ CCGAAGCTTTTGCGCCTTAAACATC 3′) for amplification of ORF ra and pair II (forward, 5′ GAATTCATGCAAAAACGTTATCTG 3′; reverse, 5′ AAGCTTTTAACGGCCTACGCGAGC3′) for amplification of ORF r. Two PCR fragments were subcloned into EcoRI-HindIII sites of pET28a(+) (Novagen) to generate the recombinant plasmids pRA and pR, and the plasmids were subsequently transformed into *E. coli* BL21(DE3). The gene homologous to ORF ra was further proved to possess OP-metabolizing activity by enzyme assay (16, 18).

Overexpression and purification of fused AKR5F1. AKR5F1 was overexpressed in *E. coli* BL21(DE3) by using the His-Bind protein fusion and purification system, which results in expression of a His-binding fusion protein. Optimal production of the fusion proteins was obtained when mid-log-phase cells (optical density at 600 nm of 0.5) were induced with 0.1 mM isopropyl-β-D-thiogalactopyranoside (IPTG) for 16 h at 30°C. Harvested cells were washed and disrupted by sonication (12), and the soluble fraction was loaded onto a His-Bind resin (Novagen). Fusion proteins were eluted with 300 mM imidazole in 50 mM Tris-HCl (pH 6.5).

Enzyme assays. Cell extracts were prepared as previously described (12). Protein concentrations were determined according to the Bradford method (Bio-Rad) using bovine serum albumin as the standard. AKR5F1 activities were measured spectrophotometrically by monitoring the absorbance at 410 nm due to the formation of a free thiol group by using Ellman's reagent (16, 18). The reactions were carried out in 50 mM Tris-HCl (pH 6.5) containing 0.3 mM malathion (or other OPs), 0.3 mM NAD(P)H, 60 μg of purified AKR5F1, and 1 mM dithionitrobenzoic acid at 28°C with β-mercaptoethanol as a standard. The reaction systems without NAD(P)H were used as the controls.

Kinetic measurement. All kinetic measurements were carried out in 50 mM Tris-HCl buffer (pH 6.5). Besides malathion, five other thion OPs, including chlorpyrifos, parathion, methyl parathion, dimethoate, and methidathion, were tested. The Michaelis-Menten kinetic constants for each substrate were obtained by measuring the initial hydrolysis rate at different substrate concentrations (0.08 to 0.8 mM) with a constant enzyme concentration of 60 μg/ml. The change in absorbance was measured with a VERSAmax microplate reader for 10 min at 30°C. All assays were performed in triplicate. The kinetic constants (K_m and k_{cat}) were calculated by the Lineweaver-Burk equation by using the Microcal origin software program.

Bioinformatic analysis. Sequence alignments were obtained with Clustal X (33) program. The putative structure for AKR5F1 was predicted as a function of the sequence homology between this protein and the data obtained from the structures of AKR2B5 previously crystallized. (AKR2B5 is a complex of xylose reductase from *Candida tenuis* [Protein Data Bank accession no. 1MI3].) The predicted structure has been generated using SwissModel (http://swissmodel.expasy.org) (10, 25, 28) and was refined with the Discover program in Insight II (2000) software package (Accelrys, Inc.). The interactions of the AKR5F1-OP-NADH complex was modeled by Docking program.

Chemicals. Malathion [*O*,*O*-dimethyl *S*-(1,2-dicarbethoxyethyl) phosphorodithioate] with 95% purity, chlorpyrifos (*O*,*O*-diethyl *O*-3,5,6-trichloro-2-pyridyl phosphorothioate) with 95% purity, parathion (*O*,*O*-diethyl *p*-nitrophenyl phosphorothioate) with 92% purity, and methyl parathion (*O*,*O*-dimethyl *O*-*p*-nitrophenyl phosphorothioate) with 86% purity were obtained from Institute for the Control of Agrochemicals, Ministry of Agriculture, China. Dimethoate (*O*,*O*-dimethyl *S*-methyl-carbamoylmethyl phosphorodithioate) with 94% purity and methidathion [*O*,*O*-dimethyl-*S*-(2-methoxy-1,3,4-thiadiazol-5 (4H)-onyl-(4)-methyl)-dithiophosphate] with 95% purity were a gift from China Agricultural University.

Nucleotide sequence accession numbers. The nucleotide sequences of the 16S rRNA and gene *akr5f1* of strain F51-1-2 have been deposited in the GenBank database under accession no. DQ277701 and DQ268871.

RESULTS AND DISCUSSION

Identification of strain F51-1-2. Strain F51-1-2 was a gram-negative, catalase-positive, oxidase-positive, and rod-shaped

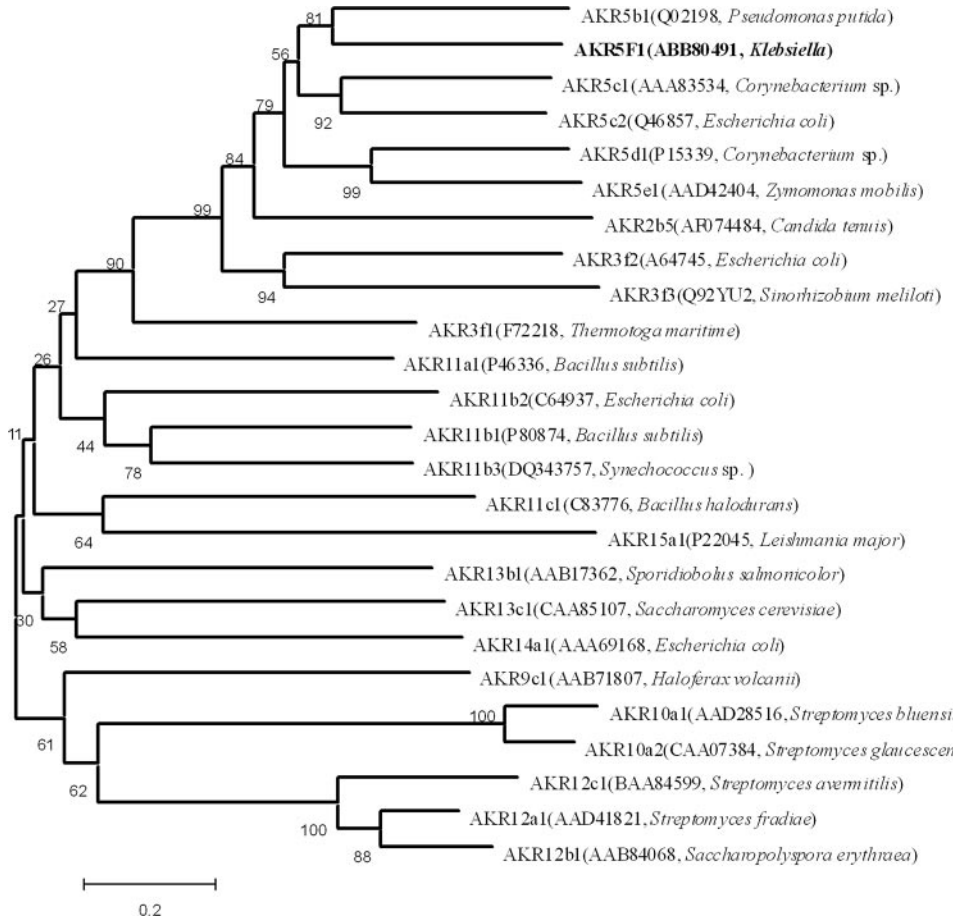

FIG. 1. Phylogenetic relationship of AKRs from bacteria. Bootstrap values obtained with 1,000 repetitions are indicated as percentages at all branches. GenBank accession numbers are given in brackets.

bacterium. The sequence of approximately 1,555 bp of the 16S rRNA gene of strain F51-1-2 was 99% identical to that of the partial sequence of 16S rRNA gene of gammaproteobacterium BAL286 (GenBank accession no. AY972873), 99% similar to that of the partial sequence of 16S rRNA gene of *Klebsiella ornithinolytica* (GenBank accession no. U78182), 99% similar to that of the partial sequence of 16S rRNA gene of *Klebsiella rennanqilfy* 18 (GenBank accession no. AY363386), and 99% similar to that of the partial sequence of 16S rRNA gene of *Klebsiella* sp. strain R-21934 (GenBank accession no. AJ786796) (calculated by using the FASTA algorithm).

The substrate utilization of strain F51-1-2 was compared with that of referred strains in the BIOLOG-GN database, and strain F51-1-2 had the greatest similarity index of 0.68 with a *Klebsiella* sp.

Cloning and expression of the *akr5f1* gene. As an enzyme assay can be used to determine the metabolism of OPs using cell extracts of strain F51-1-2, it is practical to screen the fractionated genomic library. A positive clone showing enzymatic activity was screened from the genomic library and sequenced. The sequence of the inserted fragment was 4,918 bp and contained two complete ORFs, designated as r and ra, respectively. After induction with IPTG, *E. coli* BL21(DE3) harboring pRA with ORF ra showed the reductase activity against the tested OPs but not the same cells harboring pR with ORF r, which indicated that ORF ra encoded the true reductase for OP metabolism. Sequence BLAST analysis indicated ORF ra was approximately 87% identical at the nucleotide level and 95% identical at the amino acid level to a gene

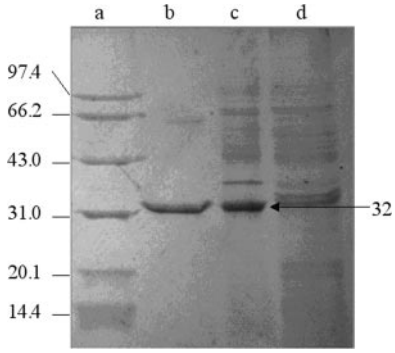

FIG. 2. Sodium dodecyl sulfate-polyacrylamide gel electrophoresis analysis of purified AKR5F1. Lane a, protein markers (kDa); lane b, purified AKR5F1; lane c, total proteins from *E. coli* BL21 cells harboring pRA with IPTG induction; lane d, total proteins from the same cells without plasmid. Purified AKR5F1 is indicated by an arrow.

TABLE 2. Kinetic constants of His-tagged AKR5F1 toward various OPs with NADH as a cofactor[a]

Substrate	V_{max} (μmol/min/mg)	Relative activity (%)	K_m (μM)	k_{cat} (min^{-1})	k_{cat}/K_m (μM^{-1} min^{-1})
Malathion	805.8 ± 51.7	100	269.5 ± 47.0	25.7 ± 1.7	0.097 ± 0.011
Methyl parathion	754.6 ± 41.7	95 ± 8	216.0 ± 32.8	24.1 ± 1.3	0.113 ± 0.011
Dimethoate	750.1 ± 18.0	93 ± 8	341.4 ± 17.3	23.9 ± 0.57	0.070 ± 0.003
Methidathion	721.7 ± 33.9	90 ± 4	252.1 ± 23.6	23.0 ± 1.1	0.092 ± 0.006
Chlorpyrifos	714.2 ± 23.6	89 ± 8	205.4 ± 25.2	22.8 ± 0.75	0.112 ± 0.011
Parathion	660.6 ± 31.2	82 ± 9	209.3 ± 4.56	21.1 ± 1.06	0.101 ± 0.003

[a] Data are mean values ± standard deviations from three independent experiments.

encoding 2,5-DKGR A (AE014075) from *E. coli* CFT073 (36). Based on sequence alignments, ORF ra was putatively identified as a member of the AKR superfamily and named *akr5f1* by the AKR superfamily website (http://www.med.upenn.edu/akr/) (17). A phylogenetic tree of strain F51-1-2 based on multiple alignments of amino acid sequences is shown in Fig. 1.

Sequence alignments of the 4,918-bp fragment of the positive clone revealed that *akr5f1* was located between nucleotides 2300 and 3151. Promoter prediction indicated that a promoter-like sequence was located upstream of the *akr5f1* ORF, and it had a typical promoter structure of TAATAA-19 nucleotides-TCTAAT. The 852-bp ORF has a putative ATG start codon 7 nucleotides downstream from a potential ribosome binding site ($^{-13}$GAAGGA^{-8}).

The high expression of His-tagged AKR5F1 fusion protein was achieved with 1 mM IPTG induction, and the fusion protein was purified with the His-Bind column. A clear band corresponding to a molecular mass of 32 kDa was observed by sodium dodecyl sulfate-polyacyrlamide gel electrophoresis (Fig. 2). Approximately 19 mg of purified protein was obtained from 500 ml of culture.

Substrate specificity of AKR5F1. In the enzyme assays, decrease in absorbance at 340 nm was monitored in the presence of NADH but not with NADPH, indicating that AKR5F1 required NADH as a cofactor and that all six of the thion OPs tested can be reduced by AKR5F1. The kinetic constants of purified AKR5F1 toward six thion OP substrates are listed in Table 2. However, the reductive products of phosphoryl (P═O) in the oxon OPs cannot be determined, so it is still unclear if the oxon OPs can be reduced by AKR5F1.

We also tried to determine the structures of the transformed products using gas chromatography-mass spectrometry (GC-MS) analysis, but the putative products were not detected by either direct injection or the derivatizing procedure. The unsteady nature of the reductive products may be responsible for the losses of signals in GC-MS analysis. OP concentrations in the assay mixtures significantly decreased, as shown by GC-MS analysis, while they did not change in the controls lacking purified AKR5F1. Moreover, the disappearance of OP substrates was coupled to NADH oxidation, as indicated by the decrease in absorbance at 340 nm (27). In contrast, no NADH oxidation was observed in the absence of OPs. More importantly, since the thiophosphoryl (P═S) is the only position that can be reduced to a free thiol group in all of the thion OP molecules tested, it's the sole position to be reduced by AKR5F1. These results clearly demonstrated that the reduction of these thion OPs by purified AKR5F1 truly occurred.

TABLE 3. Distance parameters for the interactions of AKR5F1 and OPs with NADH cofactor

OP substrate	Distance (Å)[a]		
	a1	a2	a3
Methyl parathion	2.68	3.33	2.12
Parathion	3.17	3.56	2.26
Chlorpyrifos	3.21	3.50	2.77
Malathion	2.65	3.11	2.03
Dimethoate	2.80	3.02	2.06
Methidathion	2.66	3.49	2.22
Dichlorovos	2.60	3.49	2.07

[a] a1, a2, and a3 represent the distances between the phosphorus and the 4-pro-R hydrogen of the nicotinamide ring of NADH, the thiophosphoryl sulfur and the hydroxyl hydrogen of Tyr49, and the thiophosphoryl sulfur and the amido hydrogen in His107, respectively.

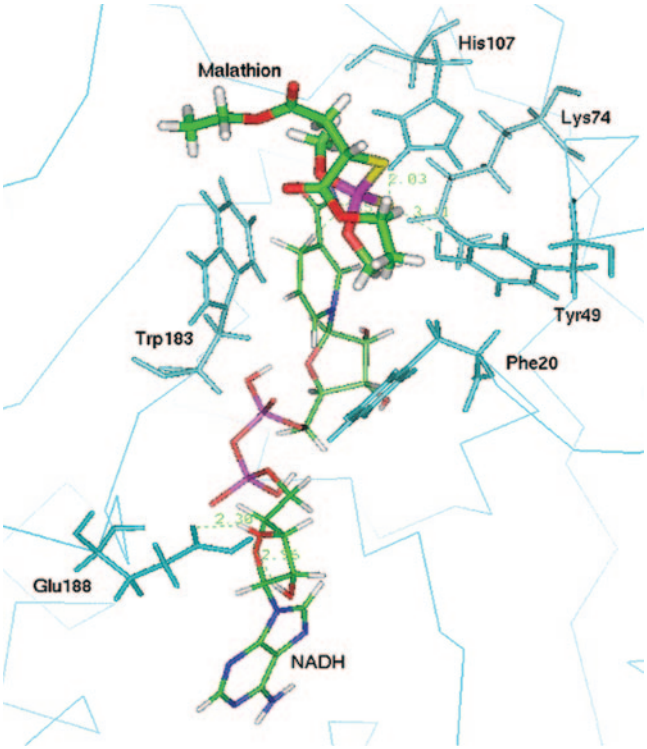

FIG. 3. Modeled three-dimensional structure of AKR5F1 from *Klebsiella* sp. strain F51-1-2 with the malathion-NADH complex. The backbone of AKR5F1 is represented in blue. The residues involved in the substrate binding pocket are highlighted by blue sticks. NADH and malathion are denoted by colored sticks. The hydrogen bonds formed between AKR5F1 and substrate are indicated by green broken lines.

FIG. 4. Sequence alignment of amino acid sequences of AKR5F1 from *Klebsiella* sp. strain F51-1-2 (NCBI accession no. DQ268871), AKR2B5 from *Corynebacterium* (NCBI accession no. AF074484), and AKR5C1 from *Candida tenuis* (NCBI accession no. M12799). The identity or similarity of residues is represented by symbols beneath the sequences, with asterisks representing the highest level of similarity, followed by colons and then periods. The residues involved in formation of the binding pocket are highlighted in gray.

The kinetic constants are not significantly different among the tested OPs. K_m is relatively higher and k_{cat} is relatively lower than those of the corresponding substrates hydrolyzed by OPH. OPH shared kinetic constants (the K_m and k_{cat} values of OPH are 50.6 ± 12.2 μM and 23.5 ± 0.2 min^{-1}, respectively, for parathion and 32.9 ± 1.7 μM and 5.46 ± 0.05 min^{-1}, respectively, for methyl parathion) (16). The OP substrates with a P—S bond such as malathion, dimethoate, and methidathion, which cannot efficiently be hydrolyzed by OPH/OPDA, can be reduced by AKR5F1. In addition, OP substrates with either a P—O bond such as parathion and methyl parathion or a P—S bond such as malathion can be reduced by AKR5F1 in moderate efficiency, suggesting that the reduction of OPs by AKR5F1 may share similar mechanism.

Structures of OPH have been well documented (34), and three pockets known as the small, large, and leaving group subsites to accommodate the phosphate substituents have been identified (4). The substrate binding pockets observed in the OPDA structure are similar to those found in OPH, except that the dimension of the large subsite in the OPDA is smaller than that of OPH (42). Due to the reduction of this subsite, OPDA processes methyl substrate more efficiently than the diethyl equivalent, while the two compounds are processed in a similar manner by OPH (3, 14, 16). Unlike OPH/OPDA, AKR5F1 has only one large pocket, which holds the *O*,*O*-dimethyl/diethyl phosphorodithioate moiety of OPs as well as NADH. The dimension of the pocket binds dimethyl-substituted substrates slightly better than diethyl-substituted substrates (Table 3). The inferences derived from structural modeling were supported by the kinetic properties of purified AKR5F1. The enzyme exhibited higher k_{cat} values for dimethyl-substituted substrates such as malathion, methyl parathion, dimethoate, and methidathion than diethyl-substituted substrates such as parathion and chlorpyrifos (Table 2).

Structure analyses. The three-dimensional putative structure of AKR5F1 from *Klebsiella* sp. strain F51-1-2 is shown in Fig. 3. The structure has been predicted on the basis of the sequence homology between this protein and AKR2B5 from *Candida tenuis* (Protein Data Bank accession no. 1MI3) previously crystallized. To investigate the similar structural char-

acteristics of AKR5F1 with AKR2B5 and AKR5C1 (2,5-DKGR A) structure, alignment of the sequence of AKR5F1 with those of AKR2B5 and AKR5C1 was performed. AKR5F1 shared 37.8% and 41% identity to AKR2B5 and AKR5C1, respectively (Fig. 4). Moreover, interactions of the OPs with the active site of AKR5F1 were docked (Fig. 3). Data showed that AKR5F1 folds into a parallel α/β-barrel consisting of eight α-helices and eight β-strands with one active pocket inside. This type of structural fold has been demonstrated in many other enzymes (8) belonging to the AKR family (15, 37, 38). In the malathion-bound structure, the *O*,*O*-dimethyl phosphorodithioate moiety of malathion and NADH interact with the active site of the enzyme, while the 1,2-dicarbethoxyethyl moiety is exposed to the solvent (Fig. 3). The thiophosphoryl sulfur makes hydrogen bond interactions with Tyr49 and His107. The residues involved in forming the catalytic pocket in AKR5F1 are almost conserved and correspond to those in AKR5C1, with the exception of Glu188, which presents a carboxylic group instead of an amidic group of Gln192 in AKR5C1, suggesting that AKR5F1 might exhibit a manner of stereo-specific reduction similar to that of AKR5C1, which proceeds via a two-step reaction mechanism involving transferring a hydride ion (H^-) from NADH to the substrate thiophosphoryl phosphorus, followed by transferring a proton (H^+) from Tyr49 or His107 to the substrate thiophosphoryl sulfur. The data of distance parameters (Table 3) suggest that other OP compounds might make similar contact with AKR5F1 and NADH as described above.

The AKRs originally were found to catalyze reduction of a wide range of ketones and/or aldehydes containing intermediates produced in many metabolic pathways and involved in the detoxification of carbonyl group-containing exogenous toxins in the environment (7). However, it has not been reported that a number of members of the AKR family can catalyze NADH-dependent reduction of thiophosphoryl (P═S). The course of evolution of AKR5F1 in bacteria remains unknown. It is unlikely that this gene/enzyme system evolved to protect against anticholinesterase compounds since bacteria do not contain acetylcholinesterases. The high identity of AKR5F1 to a number of AKRs suggests that AKR5F1 may involve in some reductive reactions associated with elementary metabolism of the microbes.

In most of the studies on microbial degradation of organophosphorus pesticides, the first reaction was hydrolysis of the phosphotriester bond (23). Conversion of thion (P═S) to oxon (P═O) OPs has also been reported (24). Recently, we found a *Bacillus* sp. strain that transforms parathion and methyl parathion by reducing the nitro group and a nitroreductase involved in the transformation (41). In the present study, we report a transformation pathway that has not been previously described: the reduction of the P═S bond of the thion OPs by *Klebsiella* sp. Moreover, we present the identification of the gene/enzyme system involved in the transformation. These results suggest that several types of reductases may play important roles in microbial degradation of organophosphates. Here, for the first time we report a novel AKR AKR5F1 that can reduce a kind of the thion OPs. The enzyme could be potentially utilized for reducing a double bond linking phosphate and sulfur in the OP molecules, which will drive the fields of both organophosphate degradation and AKR enzymology forward.

Our findings demonstrated that the novel AKR5F1 functions in OP metabolism in the presence of NADH. Moreover, the novel AKR gene involved in OP metabolism provided valuable information for exploring the course of evolution of OP metabolic genes in bacteria. Elucidation of the reductive pathway and further characterization of the enzymes involved in degradation of OPs in strain F51-1-2 represent areas for further investigation.

ACKNOWLEDGMENTS

This work was supported by grants from the Innovation Program of the Chinese Academy of Sciences (no. KSCX2-YW-G-008) and the 863 Hi-Tech Research and Development Program of the People's Republic of China (no. 2005AA601020).

We thank Wensheng Lan and Yulan Yuan for their technical assistance.

REFERENCES

1. **Atalla, A., and E. Maser.** 2001. Characterization of enzymes participating in carbonyl reduction of 4-methylnitrosamino-1-(3-pyridyl)-1-butanone (NNK) in human placenta. Chem.-Biol. Interact. **130–132:**737–748.
2. **Bauman, D. R., S. Steckelbroeck, and T. M. Penning.** 2004. The roles of aldo-keto reductases in steroid hormone action. Drug News Perspect. **17:** 563–578.
3. **Benning, M. M., S.-B. Hong, F. M. Raushel, and H. M. Holden.** 2000. The binding of substrate analogs to phosphotriesterase. J. Biol. Chem. **275:**30556–30560.
4. **Chen-Goodspeed, M., M. A. Sogorb, F. Wu, S. B. Hong, and F. M. Raushel.** 2001. Structural determinants of the substrate and stereochemical specificity of phosphotriesterase. Biochemistry **40:**1325–1331.
5. **Chow, K. C., M. P. Lu, and M. T. Wu.** 2006. Expression of dihydrodiol dehydrogenase plays important roles in apoptosis- and drug-resistance of A431 squamous cell carcinoma. J. Dermatol. Sci. **41:**205–212.
6. **Dumas, D. P., S. R. Caldwell, J. R. Wild, and R. M. Raushel.** 1989. Purification and properties of the phosphotriesterase from *Pseudomonas diminuta*. J. Biol. Chem. **261:**19659–19665.
7. **Ellis, E. M.** 2002. Microbial aldo-keto reductases. FEMS Microbiol. Lett. **216:**123–131.
8. **Farber, G. K., and G. A. Petsko.** 1990. The evolution of alpha/beta barrel enzymes. Trends Biochem. Sci. **15:**228–234.
9. **Gardiner, A. T., R. C. MacKenzie, S. J. Barrett, K. Kaiser, and R. G. Cogdell.** 1996. The purple photosynthetic bacterium *Rhodopseudomonas acidophila* contains multiple *puc* peripheral antenna complex (LH2) genes: cloning and initial characterization of four α/β pairs. Photosynth. Res. **49:** 223–235.
10. **Guex, N., and M. C. Peitsch.** 1997. SWISS-MODEL and the Swiss-Pdb-Viewer: an environment for comparative protein modeling. Electrophoresis **18:**2714–2723.
11. **Guha, A., B. Kumari, T. C. Bora, and M. K. Roy.** 1997. Possible involvement of plasmids in degradation of malathion and chlorpyriphos by *Micrococcus* sp. Folia Microbiol. **42:**574–576.
12. **Harcourt, R. L., I. Horne, T. D. Sutherland, B. D. Hammock, R. J. Russell, and J. G. Oakeshott.** 2002. Development of a simple and sensitive fluorimetric method for isolation of coumaphos-hydrolysing bacteria. Lett. Appl. Microbiol. **34:**263–268.
13. **Holt, J. G., N. R. Krieg, P. H. Sneath, J. T. Staley, and S. T. Williams.** 1994. Bergey's manual of determinative bacteriology, 9th ed. Williams and Wilkins, Baltimore, MD.
14. **Hong, S.-B., and F. M. Raushel.** 1999. Stereochemical constraints on the substrate specificity of phosphotriesterase. Biochemistry **38:**1159–1165.
15. **Hoog, S. S., J. E. Pawlowski, P. M. Alzari, T. M. Penning, and M. Lewis.** 1994. Three-dimensional structure of rat liver 3 alpha-hydroxysteroid/dihydrodiol dehydrogenase: a member of the aldo-keto reductase superfamily. Proc. Natl. Acad. Sci. USA **91:**2517–2521.
16. **Horne, I., T. D. Sutherland, R. L. Harcourt, R. J. Russell, and J. G. Oakeshott.** 2002. Identification of an *opd* (organophosphate degradation) gene in an *Agrobacterium* isolate. Appl. Environ. Microbiol. **68:**3371–3376.
17. **Jez, J. M., T. G. Flynn, and T. M. Penning.** 1997. A new nomenclature for the aldo-keto reductase superfamily. Biochem. Pharmacol. **54:**639–647.
18. **Lai, K., N. J. Stolowich, and J. R. Wild.** 1995. Characterization of P-S bond hydrolysis in organophosphorothioate pesticides by organophosphorus hydrolase. Arch. Biochem. Biophys. **318:**59–64.
19. **Lewis, D. L., D. F. Paris, and G. L. Baughman.** 1975. Transformation of malathion by a fungus, Aspergillus oryzae, isolated from a freshwater pond. Bull. Environ. Contam. Toxicol. **13:**596–601.

20. **Luccio, E. D., R. A. Elling, and D. K. Wilson.** 2006. Identification of a novel NADH-specific aldo-keto reductase using sequence and structural homologies. Biochem. J. **400:**105–114.
21. **Martin, H. J., P. U. Breyer, V. Wsol, S. Venz, S. Block, and E. Maser.** 2006. Purification and characterization of *akr1b10* from human liver: role in carbonyl reduction of xenobiotics. Drug Metab. Dispos. **34:**464–470.
22. **Matsumura, F., and G. M. Boush.** 1966. Malathion degradation by *Trichoderma viride* and a *Pseudomonas* species. Science **153:**1278–1280.
23. **Mulbry, W. W., J. S. Karns, P. C. Kearney, J. O. Nelson, C. S. McDaniel, and J. R. Wild.** 1986. Identification of a plasmid-borne parathion hydrolase gene from *Flavobacterium* sp. by Southern hybridization with *opd* from *Pseudomonas diminuta*. Appl. Environ. Microbiol. **51:**926–930.
24. **Munnecke, D. M., and D. P. H. Hsieh.** 1976. Pathway of microbial metabolism of parathion. Appl. Environ. Microbiol. **31:**63–69.
25. **Peitsch, M. C.** 1995. Protein modeling by E-mail. Bio/Technology **13:**658–660.
26. **Sambrook, J., E. F. Fritsch, and T. Maniatis.** 1989. Molecular cloning: a laboratory manual, 2nd ed. Cold Spring Harbor Laboratory Press, Cold Spring Harbor, NY.
27. **Schenzle, A., H. Lenke, P. Fischer, P. A. Williams, and H.-J. Knackmuss.** 1997. Catabolism of 3-nitrophenol by *Ralstonia eutropha* JMP 134. Appl. Environ. Microbiol. **63:**1421–1427.
28. **Schwede, T., J. Kopp, N. Guex, and M. C. Peitsch.** 2003. SWISS-MODEL: an automated protein homology-modeling server. Nucleic Acids Res. **31:**3381–3385.
29. **Serdar, C. M., D. T. Gibson, D. M. Munnecke, and J. H. Lancaster.** 1982. Plasmid involvement in parathion hydrolysis by *Pseudomonas diminuta*. Appl. Environ. Microbiol. **44:**246–249.
30. **Singh, B. K., and A. Walker.** 2006. Microbial degradation of organophosphorus compounds. FEMS Microbiol. Rev. **30:**428–471.
31. **Singh, S., and D. K. Singh.** 2003. Utilization of monocrotophos as phosphorus source by *Pseudomonas aeruginosa* F10B and *Clavibacter michiganense subsp. insidiosum* SBL 11. Can. J. Microbiol. **49:**101–109.
32. **Stormo, G. D., T. D. Schneider, and L. M. Gold.** 1982. Characterization of translational initiation sites in *E. coli*. Nucleic Acids Res. **10:**2971–2996.
33. **Thompson, J. D., T. J. Gibson, F. Plewniak, F. Jeanmougin, and D. G. Higgins.** 1997. The ClustalX windows interface: flexible strategies for multiple sequence alignment aided by quality analysis tools. Nucleic Acids Res. **25:**4876–4882.
34. **Vanhooke, J. L., M. M. Benning, F. M. Raushel, and H. M. Holden.** 1996. Three-dimensional structure of the zinc-containing phosphotriesterase with the bound substrate analog diethyl 4-methylbenzylphosphonate. Biochemistry **35:**6020–6025.
35. **Weisburg, W. G., S. M. Barns, D. A. Pelletier, and D. J. Lane.** 1991. 16S ribosomal DNA amplification for phylogenetic study. J. Bacteriol. **173:**697–703.
36. **Welch, R. A., V. Burland, G. D. Plunkett, et al.** 2002. Extensive mosaic structure revealed by the complete genome sequence of uropathogenic *Escherichia coli*. Proc. Natl. Acad. Sci. USA **99:**17020–17024.
37. **Wilson, D. K., K. M. Bohren, K. H. Gabbay, and F. A. Quiocho.** 1992. An unlikely sugar substrate site in the 1.65 Å structure of the human aldose reductase holoenzyme implicated in diabetic complications. Science **257:**81–84.
38. **Wilson, D. K., T. Nakano, J. M. Petrash, and F. A. Quiocho.** 1995. 1.7 Å structure of FR-1, a fibroblast growth factor-induced member of the aldo-keto reductase family, complexed with coenzyme and inhibitor. Biochemistry **34:**14323–14330.
39. **Xu, D., X. Liu, C. Guo, and J. Zhao.** 2006. Methylglyoxal detoxification by an aldo-keto reductase in the cyanobacterium *Synechococcus* sp. PCC 7002. Microbiology **152:**2013–2021.
40. **Yamano, S., F. Ichinose, T. Todaka, and S. Toki.** 1999. Purification and characterization of two major forms of naloxone reductase from rabbit liver cytosol, new members of aldo-keto reductase superfamily. Biol. Pharm. Bull. **22:**1038–1046.
41. **Yang, C., M. Dong, Y. L. Yuan, Y. Huang, X. M. Guo, and C. L. Qiao.** 2007. Reductive transformation of parathion and methyl parathion by *Bacillus* sp. Biotechnol. Lett. **29:**487–493.
42. **Yang, H., P. D. Carr, S. Y. McLoughlin, J. W. Liu, I. Horne, X. Qiu, C. M. J. Jeffries, R. J. Russell, J. G. Oakeshott, and D. L. Ollis.** 2003. Evolution of an organophosphate-degrading enzyme: a comparison of natural and directed evolution. Protein Eng. **16:**135–145.
43. **Zhongli, C., L. Shunpeng, and F. Guoping.** 2001. Isolation of methyl parathion-degrading strain M6 and cloning of the methyl parathion hydrolase gene. Appl. Environ. Microbiol. **67:**4922–4925.